are illustrated in Fig. 2.3.1.13(*c*). To change the range requires rotation of the X-ray tube axis or the diffractometer around *F*. The detector must also be repositioned. For forward-reflection measurements, γ is usually $\leq 10^\circ$. Extreme care must be used in the specimen preparation to avoid errors due to microabsorption (particle-shadowing) effects, which increase with decreasing γ. The 0° position cannot be measured directly and a standard is used for calibration. The range from 0° to about $15^\circ 2\theta$ is inaccessible because of mechanical dimensions. At $\gamma = 90^\circ$, only the back-reflection region can be scanned.

The aperture of the beam striking the specimen is

$$\alpha_{SB} = 2\arctan(ES_w/2a), \qquad (2.3.1.22)$$

where ES_w is the entrance slit width and *a* the distance between *F* or *F′* and the slit. The irradiated specimen length *l* is constant at all angles, $l = 2\alpha r$. A large aperture can be used to increase intensity since the specimen is close to *F*. However, the selection of α is limited if γ is small, and also because of the large flat-specimen aberration.

The receiving-slit aperture varies with the distance of the slit to the specimen

$$\alpha_{RS}(^\circ 4\theta) = 2\arctan RS_w/[2r\sin(2\theta - \gamma)]. \qquad (2.3.1.23)$$

Consequently, the resolution and relative intensity gradually change across the pattern. The *S*–*B* has greater widths at the smaller 2θ's and nearly the same widths at the higher angles compared with the θ–2θ diffractometer. The aperture can be kept constant by using a special slit with offset sides (to avoid shadowing) and pointing the opening to *C* while the detector remains pointed to *O* (Parrish *et al.*, 1967). The slit opening is tangent to FC and inclined to the beam and rotates while scanning. The constant aperture slit has

$$\alpha_{RS}(^\circ 4\theta) = 2\arctan(RS_w/2r). \qquad (2.3.1.24)$$

The axial divergence is limited by parallel slits as in conventional diffractometry and the effects are about the same. The equatorial aberrations are also similar but larger in magnitude. The specimen-aberration errors are listed in Table 5.2.7.1. The flat specimen causes asymmetric broadening; the shift is proportional to α_{ES}^2 and increases with decreasing θ. It can be eliminated by making the specimen with the same curvature as $r = FC$. In this case, one curvature satisfies the entire angular range because the focusing circle has a fixed radius. However, the curvature precludes rotating the specimen. The specimen transparency also causes asymmetric broadening and a peak shift that increases with decreasing θ. For $\mu h \rightarrow 0$, the geometric term is the same as for specimen displacement (Mack & Parrish, 1967).

The diffracted intensity is proportional to $I_0 A(\mu h) TB$, where I_0 is the incident intensity determined by α, δ, and the axial length *L* of the incident-beam assembly, $A(\mu h)$ is the specimen absorption factor, *T* the transmission of the air path, and *B* the length L_{RS} of the diffracted ring intercepted by the slit. The X-rays reflected at a depth *x* below the specimen surface are attenuated by

$$\exp\{-[\mu x\,\mathrm{cosec}\,\delta + \mu x\,\mathrm{cosec}\,(2\theta - \delta)]\}, \qquad (2.3.1.25)$$

where μ is the linear absorption coefficient. The asymmetric geometry causes the absorption to vary with the reflection angle. The air absorption path varies with the distance *O* to RS and reaches a maximum at $180^\circ + 2\gamma$. The expression for air transmission includes the radius of the X-ray tube R_T, which is needed only for the case where the X-ray tube focal line is used as *F*. In a typical instrument with X-ray tube source *F* and $r = 174$ mm, the transmission of Cu $K\alpha$ decreases from 90% at $40^\circ 4\theta$ to 62% at 210°, and Cr $K\alpha$ from 73 to 23% at the same angles.

Some of the advantages of the method include the following: (*a*) the fixed specimen makes it possible to simplify the design of specimen environment devices; (*b*) a large aperture can be used and the intensities are higher than for conventional diffractometers; (*c*) the flat-specimen aberration can be eliminated by a single-curvature specimen; (*d*) a small γ angle can be used to increase the path length *l* in the specimen, and hence the intensity of low-absorbing thin-film samples ($l = t/\sin\gamma$ and for $\gamma = 5^\circ$, $l = 11.5t$); (*e*) the method is useful in thin-film and preferred-orientation studies because about a 45° range of lattice-plane orientations can be measured and compared with conventional patterns. The limitations include (*a*) the more complicated diffractometer and its alignment, (*b*) limited angular range of about 10 to $110^\circ 2\theta$ for the forward-reflection setting, (*c*) extreme care required in specimen preparation, and (*d*) larger aberration errors.

2.3.1.4. *Reflection specimen, θ–θ scan*

In this geometry, the specimen is fixed in the horizontal plane and the X-ray tube and detector are synchronously scanned in the vertical plane in opposite directions above the centre of the specimen as shown in Fig. 2.3.1.14. The distances source to *S* and *S* to RS are equal to that the angles of incidence and diffraction and a constant $d\theta/dt$ are maintained over the entire angular range. A focusing monochromator can be used in the incident or diffracted beam. High- and low-temperature chambers are simplified because the specimen does not move. The arms carrying the X-ray tube and detector must be counterbalanced because of the unequal weights. The method has advantages in certain applications such as the measurement of liquid scattering without a covering window, high-temperature molten samples, and other applications requiring a stationary horizontal sample (Kaplow & Averbach, 1963; Wagner, 1969).

2.3.1.5. *Microdiffractometry*

There are two types of microdiffraction: (*a*) only a very small amount of powder is available, and (*b*) information is required from very small areas of a conventional-size specimen. Small-volume samples have been analysed with a conventional diffractometer by concentrating the powder over a small spot centred on a single-crystal plate such as silicon (510) or an

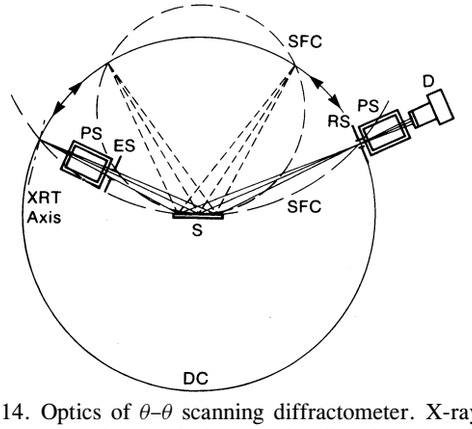

Fig. 2.3.1.14. Optics of θ–θ scanning diffractometer. X-ray tube and detector move synchronously in opposite directions (arrows) around fixed horizontal specimen. A focusing monochromator can be used after the receiving slit.

AT-cut quartz plate, or on Mylar for transmission. It is essential to rotate the specimen and increase the count time. A Gandolfi camera has also been used for very small specimens (see Section 2.3.4). A high-brilliance microfocus X-ray source has been used with a collimator made of 10 to 100 μm internal-diameter capillary tube. An *X*–*Y* stage is used with an optical microscope to locate selected areas of the specimen.

A microdiffractometer has been designed for microanalysis, Fig. 2.3.1.15 (Rigaku Corporation, 1990). It has been used to determine phases and stress in areas $< 10^4\ \mu m^2$ (Goldsmith & Walker, 1984). The key to the method is the use of an annular-ring receiving slit, which transmits the entire diffraction cone to the detector instead of a small chord as in conventional diffractometry, thereby utilizing all the available intensity. The pattern is scanned by translating the ring and detector along the direct-beam path so that

$$2\theta = \arctan(R_{RS}/L), \qquad (2.3.1.26)$$

where R_{RS} is the radius of the ring slit and L the distance from the fixed specimen. For $R_{RS} = 15$ mm, L varies from 171 to 9 mm in the transmission range 5 to 60°2θ; a 50 mm diameter scintillation counter is used. A doughnut-shaped proportional counter (3/4 of a full circle) is used for the 30 to 150° reflection specimen mode. The slit width is 0.2 mm and the aperture varies with 2θ. The intensities fall off at the higher 2θ's because of the small incidence angles to the slit. An alternative method uses a position-sensitive proportional counter. Steinmeyer (1986) has described applications of microdiffractometry.

By using synchrotron radiation (Section 2.3.2), single-crystal data for structure determination can now be obtained from a microcrystal about 5–10 μm in size; see Andrews *et al.* (1988), Bachmann, Kohler, Schultz & Weber (1985), Harding (1988), Newsam, King & Liang (1989), Cheetham, Harding, Mingos & Powell (1993), Harding & Kariuki (1994), and Harding, Kariuki, Cernik & Cressey (1994).

2.3.2. Parallel-beam geometries, synchrotron radiation

The radiation from the X-ray tube is divergent and various methods can be used to obtain a parallel beam as shown in Fig. 2.3.2.1. Symmetrical reflection from a flat crystal is the usual method. An asymmetric reflecting monochromator with small incidence angle and large exit angle expands the beam, or in reverse condenses it (§2.3.5.4.1). A channel monochromator has the advantage of not changing the beam direction. A receiving slit or preferably Soller slits can be used to define the diffracted beam. A graphite monochromator in the diffracted beam or a solid-state detector eliminates fluorescence. The incident-beam parallel slits limit vertical divergence. However, all the methods result in a large loss of intensity compared with conventional focusing. In contrast, the storage ring produces a virtually parallel beam with very small vertical divergence of about 0.1 mrad, and the monochromator is used only to select the wavelength. The rest of this section assumes a synchrotron-radiation source.

Storage-ring X-ray sources have a number of unique properties that are of great importance for powder diffraction. The advantages of synchrotron powder diffraction have been described by Hastings, Thomlinson & Cox (1984), Parrish & Hart (1987), Parrish (1988), and Finger (1989). Excellent patterns with high resolution and high peak-to-back ground ratio have been reported. These include the orders-of-magnitude higher intensity and nearly uniform spectral distribution compared with X-ray tubes, the wide continuous range of selectable wavelengths, and the single profile that avoids the problems caused by $K\alpha$ doublets and β filters. Owing to major differences in the diffractometer geometries, comparisons of intensities with X-ray tube focusing methods cannot be predicted simply from the number of source photons.

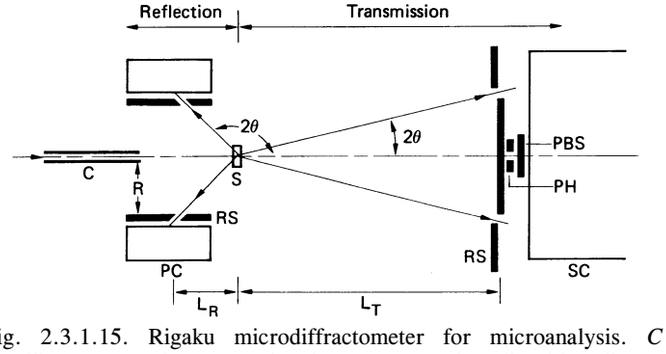

Fig. 2.3.1.15. Rigaku microdiffractometer for microanalysis. *C* collimator, PC ring proportional counter, RS ring slit with radius *r*, *S* specimen, SC scintillation counter, PBS primary beam stop, PH pinhole for alignment, *L* specimen-to-receiving-slit distance.

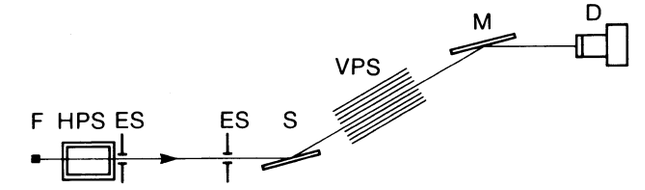

Fig. 2.3.2.1. Method to obtain parallel beam from X-ray tube for powder diffraction. HPS parallel slits to limit axial divergence, ES entrance slits (can be replaced by pair of flat parallel steel bars), *S* specimen, VPS parallel slits to define diffracted beam, *M* flat monochromator (can be omitted). *D* detector. See also Fig. 2.3.2.4(*a*).

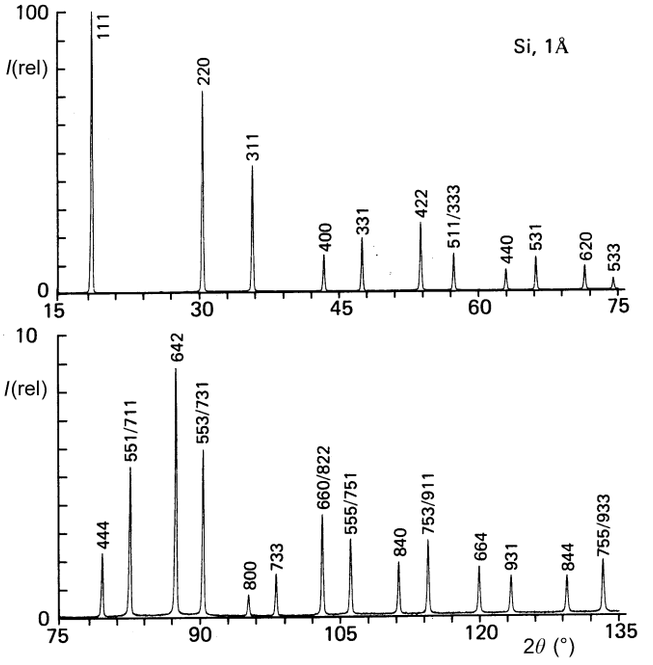

Fig. 2.3.2.2. Silicon powder pattern with 1 Å synchrotron radiation using method shown in Fig. 2.3.2.4(*a*). The 444 reflection is the limit for Cu $K\alpha$ radiation.

references